Thermal tuning of chirped SOI sidewall grating for tunable wavelength, delay, and bandwidth*

DING Jia-yue (丁嘉月), **ZOU Xi-hua** (邹喜华)**, **ZOU Fang** (邹放), **PAN Wei** (潘炜), **YAN Lian-shan** (闫连山), **and LUO Bin** (罗斌)

Center for Information Photonics & Communications, School of Information Science and Technology, Southwest Jiaotong University, Chengdu 611756, China

(Received 14 April 2020; Revised 15 May 2020)

In this work, we design a silicon-on-insulator (SOI) sidewall grating with tunable wavelength, delay, and bandwidth through thermal tuning. Incorporating uniform sidewall corrugations and a linearly chirped rib waveguide, the thermo-optic effect imposed on chirped rib waveguide changes the effective refractive index, due to the resultant of the temperature gradient. Consequently, tunable wavelength, delay, and bandwidth in SOI sidewall grating are achieved. In the numerical simulations, the designed SOI grating is demonstrated with a tunable wavelength from 1 560.7 nm to 1 561.9 nm, a tunable delay from 0 to 38 ps, and a tunable bandwidth from 1 nm to 1.5 nm.

Document code: A **Article ID:** 1673-1905(2021)04-0205-4

DOI https://doi.org/10.1007/s11801-021-0066-x

The advances in photonic integrated circuit (PIC) have promoted optical communications, microwave photonics, and optical sensing to new heights[1-3]. It can overcome the bottlenecks on bulky size, power consumption, and instability in the discrete system. Recently, a large amount of compact PIC is realized in different platforms including InP[4], Triplex[5], and silicon-on-insulator (SOI)[6]. Particularly, silicon-based photonic integration technology has a good continuity to the current mature microelectronic processing technology, because of its complementary metal oxide (CMOS) compatibility[3].

Due to the large refractive index difference of the SOI platform, waveguide Bragg gratings (WBGs) have strong refractive index modulation and thus large bandwidth via compact size and low power consumption, which is beneficial to large-scale and high-density chip integration applications[7,8]. Recently, many WBGs implemented on SOI platform have been reported. WBGs can be used as filters for wavelength selectivity[9]. Also, linearly chirped Bragg gratings (LC-WBGs) can perform pulse shaping of different wavelengths[10,11] and all-optical signal processing[12]. Meanwhile, tunable WBGs are highly desired for the optical filter[9] and dispersion compensation[13]. Electro-optical[14,15] or thermo-optical effects[16-19] can be employed to tune the spectral response and group delay of SOI gratings. For instance, the introduction of electrical tuning is able to achieve tunable delay at fixed wavelengths[15], and thermal tuning can provide tunable wavelengths and improved group delay[17,19]. These flexible tuning features enable SOI gratings to greatly reduce the cost and the redundancy of integrated chips. LC-WBGs with high tunability are essential in flexible PICs, since their tunability can be employed to combat undesired geometric variation in fabrication.

In this work, we propose an SOI sidewall grating with tunable wavelength, delay, and bandwidth by setting a thermal uniform or gradient along the device length. A tunable LC-WBG is designed and numerically demonstrated with tunable wavelength from 1 560.7 nm to 1 561.9 nm and tunable group delay from 0 to 38 ps in the uniform heating configuration. In parallel, the bandwidth can be tuned from 1 nm to 1.5 nm when applying the gradient heating. Compared with previous thermally tuned gratings, the combination of linear displacement of heaters and the chirped side-wall grating is capable of achieving high-performance tunable wavelength, group delay and bandwidth with high process tolerance. The thermally tuned sidewall grating is relatively easier to implement in the manufacturing process, which results in the grating parameters can be flexibly changed to meet different communication systems. Consequently, the tunable device is capable of implementing a compact wavelength-to-time mapping module for many specific applications, such as arbitrary waveform generator and radar signal processing[20], representatively.

The proposed grating structure is shown in Fig.1(a), which is an LC-WBG with the linearly increasing rib width. Such an LC-WBG is formed by a rib waveguide

* This work has been supported by the National Key Research and Development Program of China (No.2019YFB2203601), and the Fundamental Research Funds for the Central Universities (No.2682020ZT31).

** E-mail: zouxihua@swjtu.edu.cn

with rib etched wrinkle shape. Thanks to the etching extension on the entire inner and outer ribs, the rib formation enhances the modulation intensity and process tolerance of the grating[8,21]. The proposed LC-WBG is designed by using a thickness of 220 nm SOI substrate under a buried oxide layer with a thickness of 2 μm. The core waveguide has a silicon slab with a thickness of 150 nm and a rib height of 70 nm, which ensures a fundamental transverse-electric (TE) mode in the waveguide with a rib width of 400 nm and 700 nm, as shown in Fig.1(b). Unlike the traditional chirped grating by changing the period preciously, the chirped waveguide rib width is easier to manufacture[22].

As well known, the Bragg grating follows the Bragg equation[23], expressed as

$$\lambda_B=2n_{eff}\Lambda\ , \tag{1}$$

where λ_B is the central wavelength, n_{eff} is the effective refractive index, and Λ is the grating period.

For the rib waveguide, the effective refractive index n_{eff} varies with the rib width. In an LC-WBG, the effective refractive index is derived via the effective index method and the boundary condition. As shown in Fig.1(c), the calculated effective refractive index of the LC-WBG is linearly increasing with rib width rising from 400 nm to 700 nm. Here, Λ is setting as 300 nm with a duty cycle of 50%, and the grating is 1.8 mm in length to ensure strong reflection. In order to keep the central wavelength at 1 560 nm, the rib width is specified to be 500 nm. The rib width of its structure is changed to be 8 nm, while setting W_1=500 nm and W_2=508 nm.

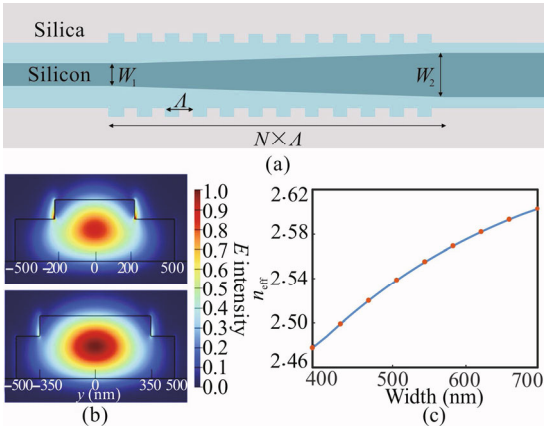

Fig.1 (a) Schematic of the linearly chirped waveguide Bragg grating; (b) Profile of fundamental TE mode in the rib waveguide with the width of 400 nm and 700 nm; (c) Effective refractive index with the width increasing from 400 nm to 700 nm

The group delay of grating τ is calculated from the phase information of the spectrum[24]

$$\tau=-\frac{\lambda_B^2}{2\pi c}\cdot\frac{d\rho}{d\lambda_B}\ , \tag{2}$$

where ρ is the phase of the corresponding wavelength. The calculated grating reflection response and group delay are shown in Fig.2(a). The central wavelength of the grating is 1 560.7 nm, and the bandwidth is 1.5 nm. The group delay gradually increases from 0 to 43 ps within the bandwidth. The grating has a chirp rate of 0.83 nm/mm and an insertion loss of 0.13 dB. Due to the wavelength selectivity of the grating, the transmission spectrum is calculated and shown in Fig.2(b).

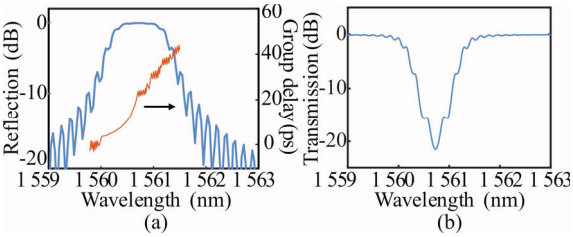

Fig.2 Characteristics of SOI chirped grating: (a) Reflection spectrum and group delay; (b) Transmission spectrum

To achieve tunable wavelength, delay, and bandwidth, the thermo-optic effect of silicon-based materials is adopted by thermally manipulating the effective refractive index of the rib waveguide. The relationship between the effective refractive index and the temperature in the thermo-optic effect[25] can be expressed as

$$n(T)=n_0+\alpha\Delta T, \tag{3}$$

where the thermo-optic coefficient α is 1.84×10^{-4}/K.

For the thermal tuning, the variations in the temperature can be implemented inside the grating by introducing the heating power or displacement from the waveguide along the propagating direction as shown in Fig.3. When the distance d between the aluminum heater and the waveguide grating is fixed at 1 μm, the temperature increases as the heater power increases. Conversely, when the heater power is fixed at 5 mW, the temperature decreases as d increases.

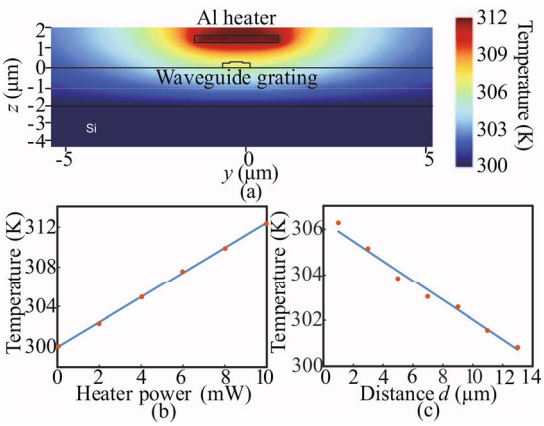

Fig.3 (a) Thermal model of the heater element above the waveguide grating; The temperature of the grating versus (b) the heater power and (c) the distance of the heater relative to the waveguide

One of the methods is the uniform heating, leading to

an identical temperature difference (i.e., ΔT) over the grating structure. For the LC-WBG, the uniform thermal tuning increases the effective refractive index by $\alpha\Delta T$. As shown in Fig.4(a), the heater is suspended above the grating, and d is 1 μm. Because the temperatures at the front end and rear end of the grating are consistent, ΔT is a stable value. Correspondingly, the change in effective refractive index with the different heating powers is shown in Fig.4(b). The effective refractive index curve increases uniformly with the rise of the heating power.

The other solution uses the gradient thermal tuning, where the higher temperature is applied to the front end and low temperature to the rear end. Since the effective refractive index at the front end is less than that of the rear end, the gradient is used to compensate the effective refractive index. Consequently, the temperature difference at a certain location $\Delta T(z)=(1-z/L_{\text{tuning}})\Delta T_0$, can be changed along the grating length, where ΔT_0 is the temperature difference at the front end, and L_{tuning} is the grating length of the gradient thermal tuning. Here, the temperature gradient coefficient is related to the distance between the heater and the grating. By varying the distance between the central axis of the heater and the waveguide, the temperature of the waveguide can be controlled as shown in Fig.4(c). With d_1=1 μm and d_2=30 μm, a specific temperature gradient can be generated in the LC-WBG. The linearly increased distance ensures that the temperature of the second half of the grating is 300 K. As shown in Fig.4(d), the effective refractive index at the front end of the grating is stable, for a given temperature gradient induced by the heater displacement. The effective refractive index at front end of the grating is 2.535 3 when the heating power is 5 mW, which is equal to in the middle of grating. Due to cancellation between the effect of the temperature gradient and waveguide width on the effective refractive index, the n_{eff} keeps invariable along the propagating direction until the rib width is increased to 504 nm.

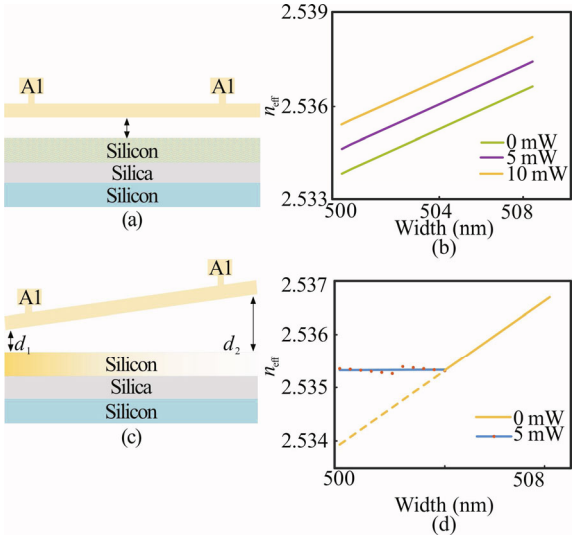

Fig.4 Side view of the (a) uniform heater position and (c) gradient heater position; The effective refractive index as a function of grating length under the (b) fixed temperature and (d) gradient temperature

Thanks to the effective refractive index change realized by the thermal tuning, the central wavelength varies in the axial direction. In the uniform tuning, the n_{eff} is increased by $\alpha\Delta T$, so the wavelength can be calculated to shift by $\alpha\Delta T\times 2\Lambda$. Since τ is related to λ_{B}, a wavelength shift results in the change of the group delay.

In this case, the bandwidth of the Bragg grating is expressed as[26]

$$\Delta\lambda_{\text{BW}}=\frac{\lambda_{\text{B}}^2}{n_{\text{group}}L}\left[1+\left(\frac{\kappa L}{\pi}\right)^2\right]^{\frac{1}{2}}, \tag{4}$$

where κ is the coupling coefficient, and L is the grating length. For the LC-WBG, $\Delta\lambda_{\text{BW}}$ is defined as the difference between two wavelengths reflected at the rear and front ends. With the gradient thermal tuning, the increase of the minimum n_{eff} causes the change of bandwidth.

To demonstrate the specifications of the designed LC-WBG, the bidirectional eigenmode expansion solver is used in our numerical simulations. The light field and phase information can be derived efficiently. Here, two thermal tuning schemes are used to achieve the corresponding changes in wavelength, delay, and bandwidth.

For the chirped grating with uniform heating, the thermal tuning changes the group delay by shifting the central wavelength. The group delay of a fixed wavelength can be changed in this way. When using the uniform heating power levels of 0, 5 mW and 10 mW, the reflection spectra and the group delay profile for the grating are measured. Fig.5(a) shows the reflection spectra of the grating with different heating power levels. As the heater power increases to 10 mW, the central wavelength is shifted to 1 561.9 nm. Meanwhile, the group delay is moving with the central wavelength as shown in Fig.5(b). For a specific wavelength (e.g., λ_{S}=1 561.2 nm), the group delay can be varied between ~0 and ~38 ps. This tunable delay can be used to flexibly change the group delay of the specific wavelength.

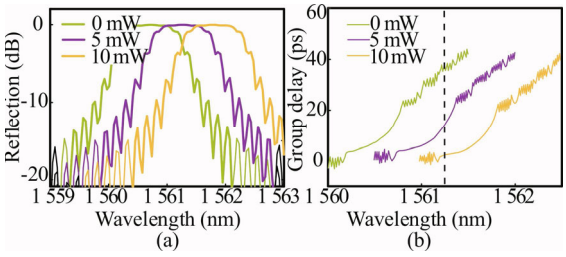

Fig.5 Uniform thermal tuning for (a) the central wavelength and (b) the group delay (The black dashed line indicates the wavelength λ_{S}= 1 561.2 nm.)

Furthermore, the variable bandwidth can be expected. In this LC-WBG, the gradient thermal tuning method is used to change the bandwidth. For instance, when the

power level is specified as 0, 2.5 mW and 5 mW for the gradient heater of the LC-WBG, the reflection spectra and the group delay profile are measured and shown in Fig.6. It is clear that the bandwidth is reduced from 1.5 nm to 1 nm, and group delay has also changed. The heating power can be adjusted to achieve a tunable desired bandwidth in the gradient thermal tuning. The device can be fabricated using CMOS-compatible technology with 193-nm deep ultraviolet lithography[22]. The heater structure formed by the resistance has been verified to adjust the local refractive index of the waveguide[27]. Due to the large mismatch between the thermal conductivity of silicon and silicon dioxide, the heater allows different temperatures for the compact structure by setting different distances[28].

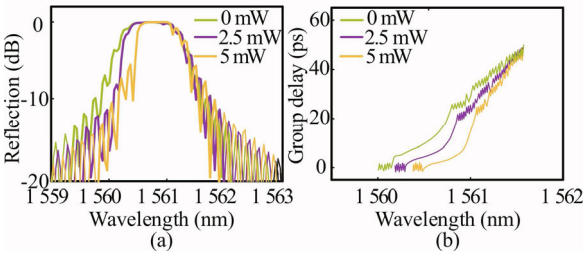

Fig.6 Gradient thermal tuning for (a) the bandwidth and (b) the group delay

In conclusion, we report a thermally tunable SOI sidewall grating, wherein different temperature distributions implemented. In the grating, linearly refractive index chirp is introduced by the change in the waveguide taper with uniform Bragg grating. The results show that the wavelength, delay, and bandwidth of the grating can be tuned through the thermo-optical effect. With the uniform thermal tuning, the wavelength can be shifted from 1 560.7 nm to 1 561.9 nm, and the group delay is tuned from 0 to 38 ps. By applying the gradient heating method, the grating bandwidth is tunable between 1 nm and 1.5 nm. It is expected that the proposed SOI grating will have wide applications in the field of on-chip optical communication and microwave photonics due to its tunable characteristics and compact size.

References

[1] B. Razavi, Design of Integrated Circuits for Optical Communications, John Wiley & Sons, 2012.

[2] D. Marpaung, J. Yao and J. Capmany, Nature Photonics **13**, 80 (2019).

[3] B. Kuswandi, J. Huskens and W. Verboom, Analytica Chimica Acta **601**, 141 (2007).

[4] JS. Fandiño, P. Muñoz, D. Doménech and J. Capmany, Nature Photonics **11**, 124 (2017).

[5] K. Wörhoff, R. G. Heideman, A. Leinse and M. Hoekman, Advanced Optical Technologies **4**, 189 (2015).

[6] D. Liang, G. Roelkens, R. Baets and J. E. Bowers, Materials **3**, 1782 (2010).

[7] X. Wang and J. Dong, Tunable Optical Delay Line Based on SOI Contradirectional Couplers with Sidewall-Rnodulated Bragg Gratings, in 2018 Progress in Electromagnetics Research Symposium, 2018.

[8] X. Wang, W. Shi, H. Yun, S. Grist, N. A. Jaeger and L. Chrostowski, Optics Express **20**, 15547 (2012).

[9] D. Oser, F. Mazeas, X. Le Roux, D. Pérez-Galacho, O. Alibart, S. Tanzilli, L. Labonté, D. Marris-Morini, L. Vivien and É. Cassan, Laser & Photonics Reviews **13**, 1800226 (2019).

[10] W. Shi, V. Veerasubramanian, D. Patel and D. V. Plant, Optics Letters **39**, 701 (2014).

[11] L. M. Rivas, J. M. Strain, D. Duchesne, A. Carballar and Azaa. José, Optics Letters **33**, 2425 (2008).

[12] M. Burla, L. R. Cortés, M. Li, X. Wang, L. Chrostowski and J. Azaña, Optics Express **21**, 25120 (2013).

[13] M. J. Strain and M. Sorel, IEEE Journal of Quantum Electronics **46**, 774 (2010).

[14] S. Khan, M. A. Baghban and S. Fathpour, Optics Express **19**, 11780 (2011).

[15] W. Zhang, N. Ehteshami, W. Liu and J. Yao, Optics Letters **40**, 3153 (2015).

[16] C. Klitis, M. Sorel and M. J. Strain, Micromachines **10**, 569 (2019).

[17] I. Giuntoni, D. Stolarek, D. I. Kroushkov, J. Bruns, L. Zimmermann, B. Tillack and K. Petermann, Optics Express **20**, 11241 (2012).

[18] J. Wang, L. Shang Guan, C. Chen, R. Cheng, C. Wang, X. Sun, Y. Wu and D. Zhang, Optical Materials Express **8**, 1870 (2018).

[19] X. Wang, Y. Zhao, Y. Ding, S. Xiao and J. Dong, Photonics Research **6**, 880 (2018).

[20] F. Zhang, J. Dong, Y. Zhu, X. Gao and X. Zhang, Integrated Optical True Time Delay Network Based on Grating-Assisted Contradirectional Couplers for Phased Array Antennas, IEEE Journal of Selected Topics in Quantum Electronics, 2020.

[21] D. Dai, Y. Tang and J. E. Bowers, Optics Express **20**, 13425 (2012).

[22] W. Zhang and J. Yao, Journal of Lightwave Technology **33**, 5047 (2015).

[23] T. Erdogan, Journal of Lightwave Technology **15**, 1277 (1997).

[24] R. Kashyap, Optics Communications **136**, 461 (1997).

[25] V. M. Passaro, F. Magno and A. V. Tsarev, Optics Express **13**, 3429 (2005).

[26] G. Jiang, R. Chen, Q. Zhou, J. Yang, M. Wang and X. Jiang, IEEE Photonics Technology Letters **23**, 6 (2010).

[27] A. H. Atabaki, A. A. Eftekhar, S. Yegnanarayanan and A. Adibi, Optics Express **21**, 15706 (2013).

[28] Piero Orlandi, Francesco Morichetti, Michael John Strain, Marc Sorel and Paolo Bassi, Optics Letters **38**, 863 (2013).